Adsorption of Zinc(II) on diatomite and manganese-oxide-modified diatomite: A kinetic and equilibrium study

Necla Caliskan *, Ali Riza Kul, Salih Alkan, Eda Gokirmak Sogut, İhsan Alacabey

Department of Physical Chemistry, Faculty of Science, Yüzüncü Yıl University, Van 65080, Turkey

ARTICLE INFO

ABSTRACT

The removal of Zn(II) ions from aqueous solution was studied using natural and MnO$_2$ modified diatomite samples at different temperatures. The linear Langmuir, Freundlich and Dubinin–Radushkevich (D–R) adsorption equations were applied to describe the equilibrium isotherms. From the D–R model, the mean adsorption energy was calculated as >8 kJ mol^{-1}, indicating that the adsorption of Zn(II) onto diatomite and Mn-diatomite was physically carried out. In addition, the pseudo-first-order, pseudo-second-order and intraparticle diffusion models were used to determine the kinetic data. The experimental data were well fitted by the pseudo-second-order kinetic model. Thermodynamic parameters such as the enthalpy (ΔH^0), Gibbs' free energy (ΔG^0) and entropy (ΔS^0) were calculated for natural and MnO$_2$ modified diatomite. These values showed that the adsorption of Zn(II) ions onto diatomite samples was controlled by a physical mechanism and occurred spontaneously.

© 2011 Elsevier B.V. All rights reserved.

1. Introduction

Inorganic contamination, especially heavy metal ions are responsible for water pollution mainly. Most of them have toxic and carcinogenic characteristics and they threaten human health and aquatic environment seriously when they enter into water. Zinc is considered as an essential element for life and acts as a micronutrient when present in trace amounts. The WHO recommended the maximum acceptable concentration of zinc in drinking water as 5.0 mg L^{-1} [1]. Heavy metal ions which occur in industrial wastewater, Zn(II) ions stand out since they are generated by industries such as mineral extraction, metal plating and battery producing [2–4]. Zinc occurs in the list of primary contaminant elements proposed by the U.S. Environmental Protecting Agency (EPA), since it has caused serious poisoning events. The main indications of zinc poisoning are desiccating muscles, imbalance of electrolytes, stomach ache, vertigo and disharmony [5]. Heavy metal ions which are dangerous to health can be removed from wastewater by known physicochemical methods [6]. Widely used methods to remove inorganic and organic wastes which cause environmental pollution and harm human health involve chemical precipitation, membrane filtration, ion exchange, coagulation and adsorption [7,8]. Adsorption is one of the methods used in removing heavy metals from aqueous solutions. Natural or modified diatomite (chemically or thermally) has already been used for the adsorption of different elements from water and wastewaters [9].

Diatomite (SiO$_2$·nH$_2$O) is a soft, light-color slightly sedimentary rock formed from accumulation of siliceous crusts of diatoms, which are aquatic organism from algae, and have fossil characteristics [10]. It is used in many industrial areas as filtering-utility material, filling material, insulation material, adsorbent, abrasive material and surface cleaning material, catalyst carrier, light construction material and silica source in chemical material manufacturing because of its physical and chemical characteristics [10,11]. Its usage for filtering is highly prevalent because of its porous structure, low density, high surface area, chemical inertness and being sterile [12].

Active centers of diatomite having active hydroxyl groups on its surface responsible for adsorption may be characterized as the following: (i) insulated free silanol groups (–SiOH), (ii) free dual silanol group (–Si(OH)$_2$), (iii) –Si–O–Si bridges with oxygen atoms on the surface. Silanol groups are active and have a tendency to react with many polar organic compounds and various functional groups [13]. Therefore, they are used as adsorbent in heavy metal and dye prevalently. Adsorption capacity and filtration rate of diatomite have been improved by thermal process and various chemical applications. One of these processes is to change surface characteristics of diatomite by modifying it with MnO$_2$ (Mn-diatomite). Manganese oxides were impregnated onto diatomite to form the type known as δ-birnessite. Manganese oxides are an important material in terrestrial, marine geochemistry and in sediments. The birnessite-type

---

$(Na_4Mn_{14}O_{27}\cdot9H_2O)$ or $(\delta\text{-}MnO_2)$ is one of the most active and common forms of mineralised manganese in soil, sediments, and water. It is a strong adsorbent of mineral ions and acts as a scavenger in marine and freshwater environments [14]. Adsorption capacity of Mn-diatomite for metal cations is higher than that of natural diatomite depending on its high negative surface charge [15].

The aim of the present investigation was to study the sorption mechanism of Zn(II) ions onto natural and MnO_2-modified diatomite, and to determine the equilibrium and kinetic parameters of the process. With this aim in mind, sorption isotherms have been measured at different temperatures and the Langmuir, Freundlich and Dubinin–Radushkevich (D–R) model parameters and the thermodynamic parameters determined. The kinetic adsorption results have been analyzed using pseudo-first-order, pseudo-second-order reactions and intra-particle diffusion model, respectively.

2. Materials and method

2.1. Materials

The raw diatomite used in this study was collected as a natural resource from Çaldıran region of Lake Van Basin in East Anatolia (Turkey). Quantitative chemical analysis of diatomite obtained by XRF technique revealed that the Çaldıran-Van diatomite consists mainly of SiO_2 (69.70%), and it has 11.50% Al_2O_3, 4.40% Fe_2O_3, 0.65% TiO_2, 0.80% Na_2O, 1.40% K_2O and 11.55% loss on ignition.

Natural diatomite sample, which was powdered by pounding in a porcelain mortar, was washed by distilled watered and dried in a drying oven at 105 °C and then, it was put into polyethylene bags and stored to use in the future.

2.1.1. Surface modification

15 g diatomite was mixed with 6 M NaOH at 80 °C for 2 h. The mixture into which $MnCl_2$ was added by keeping its pH between 1 and 2 by using HCl was kept in mixing for 10 h at room temperature. For making manganese hydroxide formation rate increase, the diatomite was re-mixed with 6 M NaOH at room temperature for 10 h and then, decanted and left subject to air for oxidation. The sample was washed by distilled watered and dried in a drying oven at 105 °C and then, it was powdered by pounding in a porcelain mortar. It was put into polyethylene bags with "Mn-diatomite" label and stored to use in the future [15].

All the chemicals employed were analytically pure and experiments were conducted using Zn(II) salt solutions. For this purpose, a stock solution containing 1000 mg L^{-1} Zn(II) ions was prepared by dissolving the appropriate amount of $Zn(NO_3)_2$ (Merck) in 1 L of doubly distilled water.

2.1.2. Sample characterization

During characterization of natural diatomite and modified diatomite samples, X-ray fluorescence spectrometer (XRF, Philips 2400) was used for chemical analysis. Thermal analysis (TG–DTA) was carried out using Rigaku 2.22E1 Thermal Analyzer under the following operational conditions: heating from 10 to 1099 °C at a rate of 20 °C min^{-1} in atmospheric air. Fourier-transform infrared (FT-IR) measurement was mounted on a Bio-Rad Win-IR spectrometer at a resolution of 2 cm^{-1} in KBr pellet at room temperature. For mineralogical analysis, X-ray diffraction (XRD) pattern of diatomite were recorded with a Philips PW 1830-40 X-ray diffractometer with a Cu-K_α radiation. The chemical composition of the natural diatomite and modified diatomite were examined using scanning electron microscopy (model: LEO 440 computer controlled digital).

The surface area of the diatomite was determined, according to Sears' method [16], by weighing 1.5 g of diatomite, and acidifying with dilute hydrochloric acid to pH of 3–3.5. Sodium chloride (30 g) was then added with stirring, and the mixture was made up to a total volume of 150 mL with distilled water. The solution was titrated with 0.10 M sodium hydroxide and the pH measured throughout the titration process. The volume, V, required to increase the pH from 4 to 9 was recorded. The surface area (S) was estimated from the equation [15]:

$$S\,(m^2\,g^{-1}) = 32V - 25$$

where 32 and 25 are Sears empiric constants.

The pH at which the sorbent surface charge takes a zero value defined as point of zero charge (pH_{pzc}) was determined by potentiometric titrations with 0.1 M HNO_3 solution of different masses of diatomite material (0.15, 0.30, and 0.45 g) suspended in 0.03 M KNO_3 solution [17].

Moreover, thin cross-sectional analysis applied on the diatomite rock collected from Çaldıran-Van region.

2.1.3. Adsorption

Natural and Mn-diatomite samples were grinded in separate mills. Then, particle size was lowered by the help of 230-mesh sieve. The adsorption characteristics of Zn(II) ions were examined by mixing 0.1 g of the original diatomite sample and the Mn-diatomite sample with 10 mL of $Zn(NO_3)_2$ solutions whose initial concentrations (C_i) were 5 mg L^{-1}, 10 mg L^{-1} and 15 mg L^{-1}, respectively. The resulting mixtures were shaken in a thermally controlled automatic shaker at 110 rpm at temperatures of 298 K, 303 K and 313 K for different time periods until equilibrium conditions had been attained. The concentrations of the ions remaining in the aqueous solutions after adsorption were measured via a Solaar AA M series v1, 23 model (Thermo Scientific, UK) atomic absorption spectrophotometer.

Measurements of the pH values of the natural and modified diatomite suspensions were determined by using a WTW pH meter (Series 720, Germany).

2.2. Equilibrium adsorption studies

Initial experiments showed that the time period necessary for equilibrium to be attained in the Zn(II) ion/diatomite systems was 120 min, since after this time the amount of metal ions adsorbed did not change significantly with time. Optimum conditions for the adsorption process were ascertained by studying the various parameters influencing the same. Thus, it was established that the adsorption capacity changed according to the initial concentration of the Zn(II) ion solution employed and the temperature. In such equilibrium studies, it is essential to determine the adsorption capacity of adsorbent and, especially, define the adsorption isotherm constants that are important in clarifying the surface characterics of the adsorbent. In the present work, these studies were undertaken using the batch adsorption technique. The quantity of Zn(II) ions adsorbed per unit amount of adsorbent (q_e) was calculated from the relationship:

$$q_e = \frac{(C_i - C_e)V}{m} \tag{1}$$

where C_i is the initial concentration of the Zn(II) ion solution, C_e is the concentration of Zn(II) ions present at equilibrium (mg L^{-1}), V is the volume of the solution (L) and m is the mass of adsorbent employed (mg).

2.3. Kinetic adsorption studies

For such studies, 0.1 g of natural or modified diatomite was shaken with 10 mL of a Zn(II) ion solution of a known initial concentration. Samples were taken from the solution at known time intervals over a total period of 120 min, viz. the time necessary

to achieve equilibrium, and analyzed by atomic absorption spectrophotometry. Adsorption experiments were conducted by using three different initial concentrations of Zn(NO$_3$)$_2$ solution, viz. 5, 10 and 15 mg L^{-1}, respectively. The amounts of Zn(II) ions adsorbed at various time periods (q_t) were calculated via Eq. (2):

$$q_t = \frac{(C_i - C_t)V}{m} \tag{2}$$

where C_t is the concentration of Zn(II) ions present in the aqueous solution after t min. All other quantities in this equation have the same meanings as in Eq. (1).

2.4. Equilibrium adsorption isotherm models

In this study, the Langmuir, Freundlich and Dubinin–Radushkevich (D–R) isotherms were applied to describe the equilibrium between adsorbed Zn(II) ions and those remaining in the aqueous solution. The Langmuir isotherm equation is valid for monolayer sorption onto surface containing a finite number of identical sorption sites, and may be described in a linear form by the relationship [9]:

$$\frac{1}{q_e} = \frac{1}{K_L V_m} \times \frac{1}{C_e} + \frac{1}{V_m} \tag{3}$$

where q_e (mg g^{-1}) and C_e (mg L^{-1}) are the amounts adsorbed and remaining in solution at equilibrium, respectively, V_m is the monolayer capacity and K_L is the equilibrium constant which can be determined via the linearized Langmuir isotherm.

Another important parameter, R_L, known as the separation factor, could be obtained from the relation:

$$R_L = \frac{1}{1 + K_L C_{ref}} \tag{4}$$

where C_{ref} is any equilibrium liquid phase concentration of the solute. It has been established that (i) $0 < R_L < 1$ for favourable adsorption, (ii) $R_L > 1$ for unfavourable adsorption, (iii) $R_L = 1$ for linear adsorption, and (iv) $R_L = 0$ for irreversible adsorption [18].

The Freundlich equation is a purely empirical relationship based on sorption onto a heterogeneous surface. This model, which has proved to be satisfactory for low concentrations and often represents an initial surface adsorption followed by a condensation effect, resulting from extremely strong solute–solute interaction [9]. Its linear form is commonly represented as:

$$\log q_e = \log K_F + \frac{1}{n} \log C_e \tag{5}$$

Although this equation was initially derived for adsorption from solution, it can also be used for adsorption from the gaseous or vapour phase, employing pressures rather than concentrations. In this equation, K_F [(mg g^{-1})(mg L^{-1})^n] and n are the Freundlich constants related to adsorption capacity and adsorption intensity, respectively [2].

The Langmuir and Freundlich isotherms are deficient to clarify the physical and chemical characteristics of adsorption. The D–R isotherm is more general than the Langmuir isotherm, because it does not assume a homogeneous surface or constant sorption potential. The D–R equation is [19]:

$$\ln q_e = \ln V'_m - K'_{\varepsilon^2} \tag{6}$$

where, q_e is the removed heavy metal amount per unit clay (mg g^{-1}), V'_m is D–R adsorption capacity (mg g^{-1}), K' is the constant related to adsorption energy (mol^2 kJ^{-2}), ε is Polanyi potential. The Polanyi potential (kJ mol^{-1}) ε is written as

$$\varepsilon = RT' \ln \left(1 + \frac{1}{C_e}\right) \tag{7}$$

In this equation, R is gas constant (kJ K^{-1} mol^{-1}) and T' is temperature (K).

The sorption energy E (kJ mol^{-1}) gives information about physical chemical characteristics of adsorption. The magnitude of E is between 8 and 16 kJ mol^{-1}, the sorption process follows chemical ion-exchange, while for the values of $E < 8$ kJ mol^{-1}, the sorption process is of a physical nature [2]. The mean free energy of the adsorption E is

$$E = (-2K')^{-0.5} \tag{8}$$

2.5. Kinetic models

For the interpretation of the kinetic batch experimental data three different kinetic models were used: (1) the pseudo-first order kinetic model (Eq. (9)) [20–22], (2) the pseudo-second order kinetic model (Eq. (11)) [21,23,24] and (3) the intraparticle diffusion model (Eq. (13)) [9].

2.5.1. Pseudo-first-order kinetic equation

This well-known kinetic equation was first extensively employed by Ho and McKay [25] and may be expressed as:

$$\frac{dq_t}{dt} = k_1(q_e - q_t) \tag{9}$$

where q_e and q_t are the amount of solute adsorbed per unit amount of adsorbent at equilibrium and any time, t, respectively (mg g^{-1}) and k_1 is the pseudo-first-order rate constant (min^{-1}). Integrating Eq. (9) employing the boundary conditions that at $t = 0$, $q_t = 0$, and that at $t = t$, $q_t = q_t$, the linear form of the equation become:

$$\ln(q_e - q_t) = \ln q_e - k_1 t \tag{10}$$

The adsorption rate constant, k_1 (min^{-1}), can be obtained from the slope of the linear plot of $\ln(q_e - q_t)$ versus t.

2.5.2. Pseudo-second-order equation

The pseudo-second order kinetic equation is:

$$\frac{dq_t}{dt} = k_2(q_e - q_t)^2 \tag{11}$$

where k_2 is the pseudo-second-order rate constant [g mg^{-1} min^{-1}]. On integration, employing the conditions that at $t = 0$, $q_t = 0$ and that at $t = t$, $q_t = q_t$, this equation can be re-arranged to give the linear form:

$$\frac{t}{q_t} = \frac{1}{k_2 q_e^2} + \frac{t}{q_e} \tag{12}$$

The plot of t/q_t versus t gives a linear relationship, which allows the values of q_e and k_2 to be computed [26].

2.5.3. Intraparticle diffusion model

The variation in the extent of adsorption with time at different initial metal ion concentrations was processed for evaluating the role of diffusion in the adsorption system [18]. Intraparticle diffusion model equation is:

$$q_t = x_i + k_i t^{1/2} \tag{13}$$

where k_i is the intra-particle diffusion rate constant (mg g^{-1} min$^{-0.5}$). The value of k_i can be obtained by plotting q_t against $t^{1/2}$.

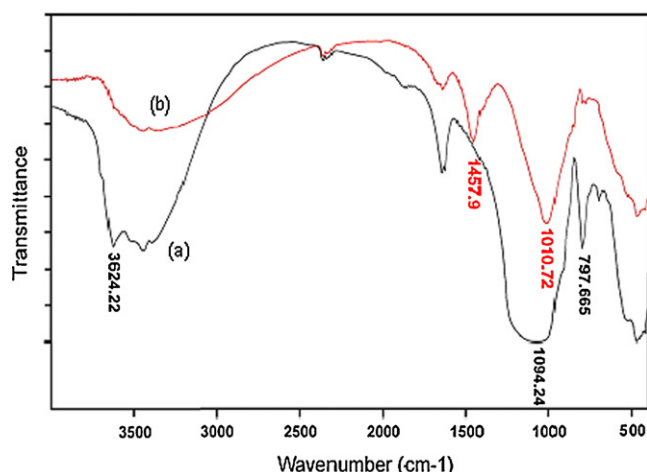Fig. 1. FT-IR spectrum of diatomite (a) and Mn-diatomite (b) sample.

Fig. 2. TG–DTA curve of diatomite sample.

2.6. Thermodynamic parameters

The thermodynamic behaviour of Zn(II) ion adsorption onto natural and modified diatomite was evaluated employing the following equations:

$$K_d = \frac{C_i - C_e}{C_e} \frac{V}{m} \tag{14}$$

$$\ln K_d = \frac{\Delta S^0}{R} - \frac{\Delta H^0}{RT} \tag{15}$$

where C_i is the initial concentration (mg L^{-1}), C_e is the equilibration concentration after centrifugation (mg L^{-1}), V is the volume (mL) and m is the mass of diatomite (g), R (8.314 J mol^{-1} K^{-1}) is the ideal gas constant, and T (K) is the temperature in Kelvin. ΔH^0 is the enthalpy change and ΔS^0 is the entropy change in a given process. The values of enthalpy (ΔH^0) and entropy (ΔS^0) can be calculated from the slope and y-intercept of the plot of $\ln K_d$ versus $1/T$ via applying the equations [27].

Free energy changes (ΔG^0) of specific adsorption are calculated from:

$$\Delta G^0 = \Delta H^0 - T\Delta S^0 \tag{16}$$

3. Results and discussion

3.1. Characterization of the adsorbent

The surface area of diatomite was estimated by using simple and rapid Sears' method. Even though this method was developed mainly for pure silica, it can also be applied for samples containing high silica content. According to this method, the estimation of surface area depends mainly on the hydroxyl groups present on the surface. The surface area of diatomite used in this study was calculated as 48 m^2 g^{-1}.

FT-IR analysis was carried out in the range 400–4000 cm^{-1}, in order to investigate the surface characteristics of diatomite and Mn-diatomite. The FT-IR spectrums of diatomite show major adsorption bands at 3624, 1625, 1094 and 797 cm^{-1}, as depicted in Fig. 1. The band at 3624 cm^{-1} is due to the free silanol group (SiO–H) on the surface, the band at 1625 cm^{-1} represents H–O–H bending vibration of water, the band at 1094 cm^{-1} may be attributed to siloxane (–Si–O–Si–) group stretching and the peak at 797 cm^{-1} may correspond to SiO–H vibration [28–30]. It is seen that the densities disappeared in the bands of 3624 and 1094 cm^{-1} after modification as a result of chemical interaction between silanol group on the surface and oxides. The bands of 1457 and 1010 cm^{-1} are Si–O

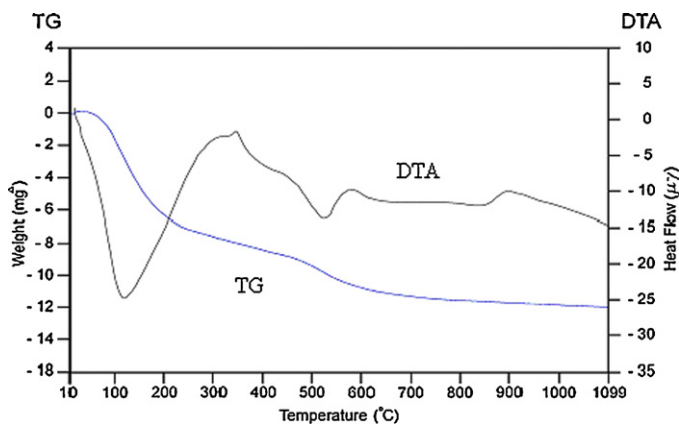tension bands [31,32]. Disappearing of OH bands after modification indicates that modified is well.

The dehydration temperatures, the corresponding weight losses, and the thermal effects were determined from the DTA and TG curves. The diatomite surface contains a large amount of free and bound water firmly bonded to the surface. During the condensation of hydroxyl groups on the diatomite surface, the dehydration process can be separated into the two stages. The first stage represents the dehydration of water adsorbed by the surface, and the second stage is the condensation of hydroxyl groups on the surface and simultaneous removal of water adsorbed on the surface of macropores and micropores. The condensation of hydroxyl groups and dehydroxylation occur simultaneously, and, finally, water and hydroxyl groups located on the inner surface of micropores are lost. A typical TG–DTA curve for the diatomite is shown in Fig. 2. The TG curve exhibits two distinct weight loss steps and the DTA curve showed two endothermic peaks and one exothermic peak. In the first step, diatomite shows weight loss of about 8.9% up to 522 °C, which is accompanied by two endothermic peaks at around 100 and 500 °C in the DTA curve, probably due to dehydration and dehydroxylation, respectively. The second weight loss step of 2.4% above 550 °C corresponds to the collapse of all macropores, which is accompanied by one exothermic peak at around 900 °C [32,33].

The X-ray powder diffraction results of natural and the Mn-diatomite mineral are shown in Fig. 3a and b. The diffraction spectrogram indicates that the diatomite consists mainly of silica (SiO$_2$) with smaller amounts of Al$_2$O$_3$, Fe$_2$O$_3$, TiO$_2$, Na$_2$O, and K$_2$O. The amorphous band, shown in Fig. 3a is probably due to the glass formation of SiO$_2$ [34].

Microphotographs of diatomaceous earth and modified diatomite are presented in Fig. 4a and b. The diatomite sample is composed of plaque and circular-shape diatom particles with sizes of 0.005–0.025 mm in clay matrix according to the microphotographs and thin cross-sectional analysis applied on the diatomite rock taken from the region.

As it is shown in Fig. 4b, the diatomite surface is covered by cluster forms after modification. The clusters sizes range from one to several micrometers in size.

3.2. Adsorption of Zn(II) ions onto diatomite samples

The pH of the adsorbate solutions is an important parameter governing adsorption on different adsorbents. In the present study, pH values of the natural and modified diatomite suspensions were measured 7.26 and 7.54, respectively. The solubility product for Zn(II) ions indicates that precipitation of Zn(OH)$_2$ will occur at pH > 8 [35]. Zinc(II) occurs predominantly as Zn^{2+} ion species up to a pH of ~7.5, but at higher pH values their concentration decreases.

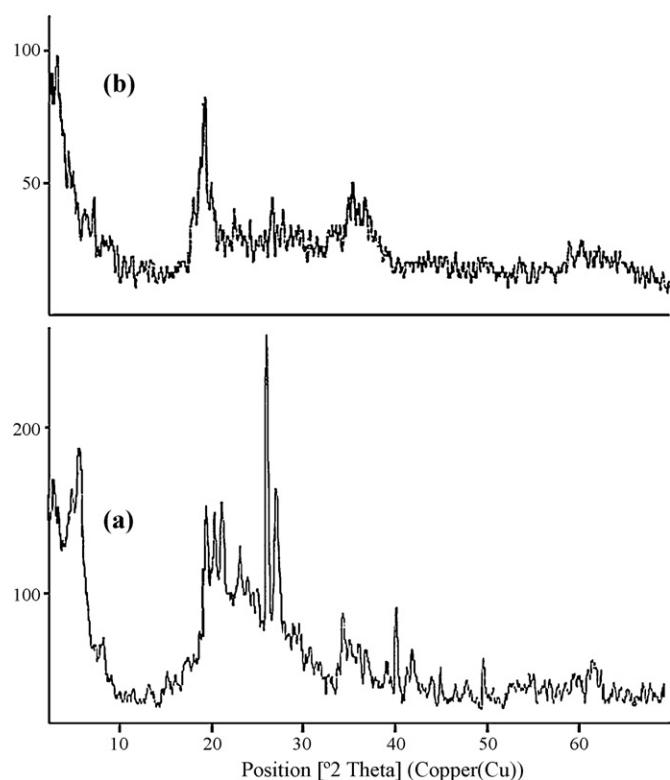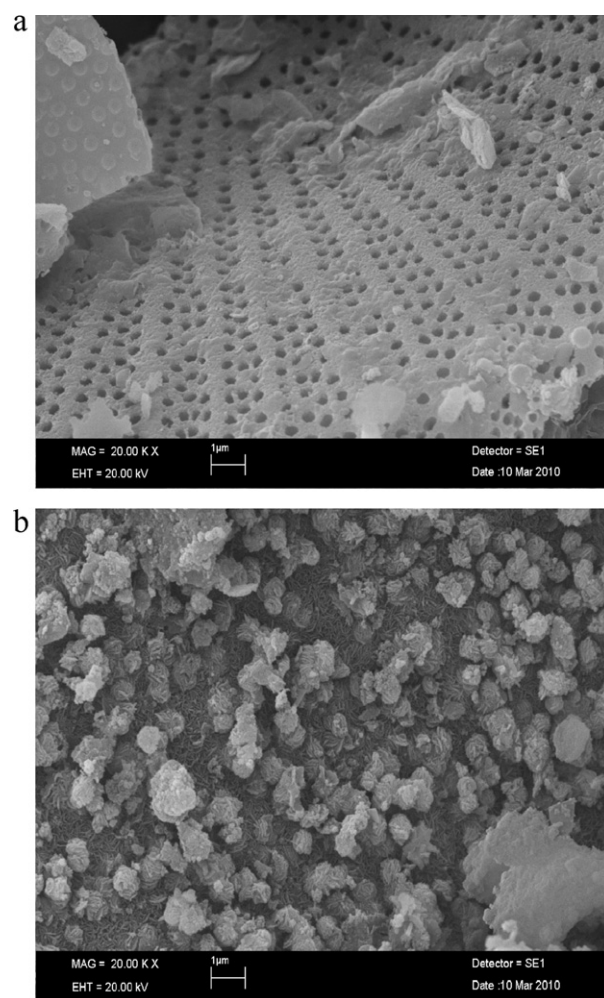**Fig. 3.** X-ray patterns of the (a) natural diatomite and (b) Mn-diatomite.

Fig. 4. (a) Scanning electron microphotograph of the diatomite and (b) scanning electron microphotograph of the Mn-diatomite.

At such pH values, the concentrations of $ZnOH^+$ and $Zn(OH)_2(aq)$ increase, with other Zn species [$ZnNO_3^+$, $Zn(NO_3)_2(aq)$, $Zn(OH)_3^-$, $Zn(OH)_4^{2-}$ and $Zn_2(OH)^{3+}$] occurring in negligible concentrations [36]. At pH < 7.5, the main species is Zn^{2+} and the removal of Zn^{2+} is mainly accomplished via adsorption reaction.

Surface charges of diatomite may form by chemical reactions on the surface depending on ionizable functional groups such as –OH, –COOH, –SH [37]. In case of oxides and hydroxides, the surface is charged by [$SiOH_2^+$] and [SiO^-] ionizations. This is called as surface charge density. Surface charge density depends on pH of the media. The charges from cations and anions are equal and total charge is zero at zero charge point. Hydroxyl groups on the surface of the diatomite may gain or lost proton by changing of pH. The surface gains proton and is charged positively at low pH values.

$$\equiv Si-OH + H^+ \rightarrow \equiv Si-OH_2^+ \tag{i}$$

Hydroxides on the surface lost proton and the surface is charged negatively at high pH values.

$$\equiv Si-OH + OH^- \rightarrow \equiv Si-O^- + H_2O \tag{ii}$$
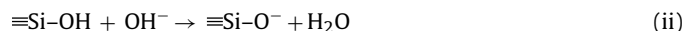
When the solution pH was above the pH_{pzc}, the diatomite surface had a negative charge, while at low pH (pH_{pzc}) it has a positive charge [38].

The pH_{pzc} was identified as the pH where 0.1 M HNO_3 titration curves of different adsorbent masses (0.15, 0.20, and 0.45 g suspended in 0.03 M $NaNO_3$ at pH 12.0) converged with that of the reactive blank solution [39]. The pH_{pzc} obtained was ~3.70 for diatomite, thus the diatomite surface may also be negatively charged, providing adsorption sites for Zn^{2+} ions.

Considering that active center for adsorption is SiO_2, diatomite surface charge is given as zero at pH ~ 3.7 and Mn-diatomite's surface charge is given as $-40\,\mu coul\,cm^{-2}$ [15,40]. Surface charge of MnO_2 is higher than those of other oxides such as SiO_2, TiO_2, Al_2O_3 and FeOOH depending on its high acidity constant. The surface is ionized at low pH values and it is charged more negatively compared with other oxides [15].

Initial concentration provides an important driving force to overcome all the mass transfer resistance of Zn(II) between the aqueous solution and the diatomite surface. As a result, high initial Zn(II) concentration will enhance the adsorption process [38]. The effects of the initial solution concentration on the adsorption of Zn(II) ions onto natural and modified diatomite are shown in Fig. 5a and b, where the initial Zn(II) ion concentrations employed were 5, 10 and 15 mg L^{-1}, respectively. The amount of Zn(II) ions adsorbed (q_e) was calculated from the experimental data via Eq. (1). As can be seen from the figures, the adsorption capacities of the natural and modified diatomite towards Zn(II) ions increased linearly with increasing initial concentrations of these ions. Besides, the amount of Zn(II) ions adsorbed onto modified diatomite was higher than onto the natural material.

The effect of temperature on the adsorption of Zn(II) ions from an aqueous solution of 5 mg L^{-1} initial concentration onto natural and modified diatomite studied is depicted in Fig. 6a and b. In all cases, the amount of Zn(II) ions adsorbed increased with temperature, indicating that the process was endothermic in nature.

The effect of the contact time on the adsorption of Zn(II) ions onto the natural and modified diatomite samples studied is illustrated in Fig. 7, where measurements were undertaken over a period of 5–180 min. In all cases, a contact time of 120 min was sufficient to ensure that adsorption equilibrium had been attained.
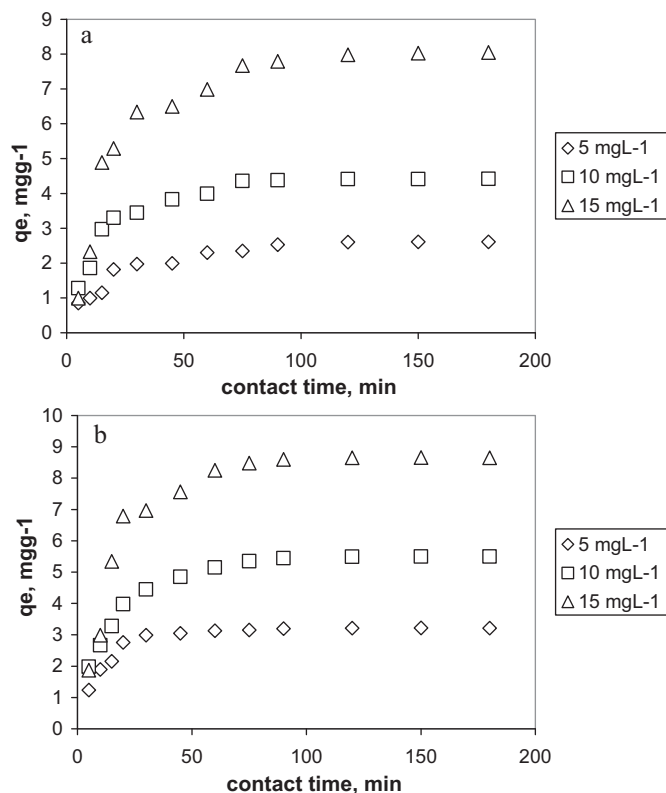
Fig. 5. (a) Effect of initial concentration for kinetic adsorption of Zn^{2+} on diatomite at 298 K and (b) effect of initial concentration for kinetic adsorption of Zn^{2+} on Mn-diatomite at 298 K.
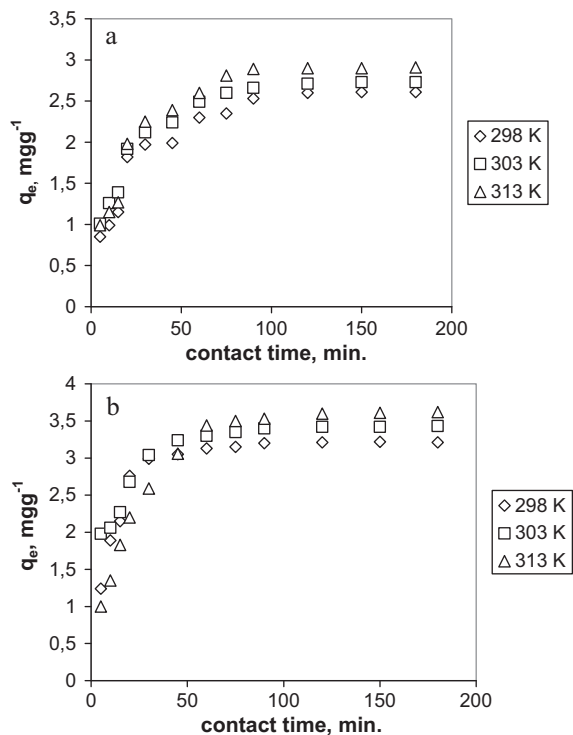

Fig. 6. (a) Effect of temperature for kinetic adsorption of Zn^{2+} onto natural diatomite at 5 mg L^{-1} initial zinc concentrations and (b) effect of temperature for kinetic adsorption of Zn^{2+} onto Mn-diatomite at 5 mg L^{-1} initial zinc concentrations.

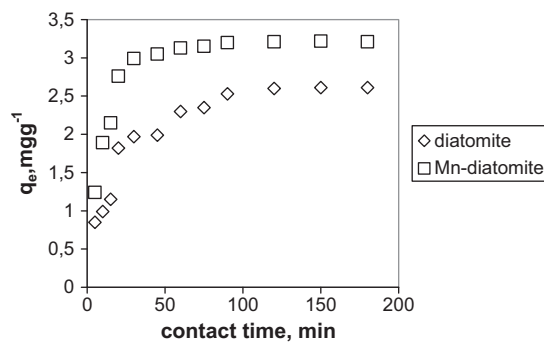**Fig. 7.** Effect of contact time for the adsorption of Zn(II) on natural and modified diatomite in 5 mg L^{-1} initial zinc concentration at 298 K.

For this reason, in subsequent experiments, 120 min was chosen as the optimum contact time. It can be attributed to the fact that at the initial stage the adsorption sites are more, and the metal ions can interact easily with the sites, so a higher adsorption rate is obtained. Besides, the driving force for adsorption is the concentration gradient between the bulk solution and the solid–liquid interface, and the concentration gradient is higher in the initial period, which results in a higher adsorption rate. The slow adsorption rate in later stage is due to slower diffusion of solute into the interior of the adsorbent [41].

3.3. Adsorption isotherms

The experimental data were applied on Langmuir, Freundlich and D–R adsorption models successively, using Eqs. (3), (5) and (6). The Langmuir plot supplied the graphic of $1/q_e$ versus $1/C_e$ has been given in Fig. 8a and b.

The Freundlich plots of $\log C_e$ versus $\log q_e$ has been given in Fig. 9.
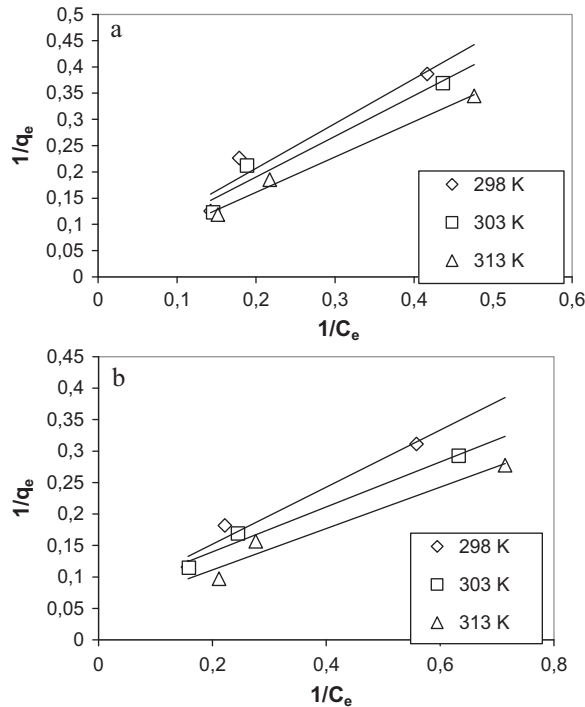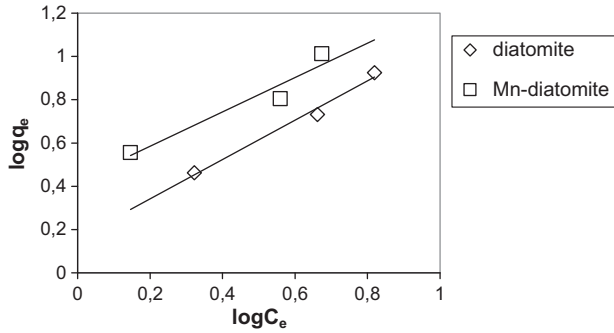

Fig. 8. (a) Langmuir plots for the adsorption of Zn(II) ions onto natural diatomite various temperatures and (b) Langmuir plots for the adsorption of Zn(II) ions onto Mn-diatomite at various temperatures.

Table 1
Langmuir, Freundlich and D–R isotherm constants for the adsorption of Zn(II) ions on natural and modified diatomite at different temperatures.

| Adsorbent	T (K)	Langmuir isotherm constants			Freundlich isotherm constants			D–R isotherm constants			
		V_m (mg g^{-1})	K_L	R^2	K_F	n	R^2	K' (mol^2 kJ^{-2})	V_m' (mg g^{-1})	E (kJ mol^{-1})	R^2
Natural diatomite	298	27.247	0.0430	0.9275	1.171	1.124	0.9740	−0.1418	7.297	1.877	0.7906
	303	27.777	0.0465	0.9485	1.213	1.088	0.9146	−0.1267	7.599	1.986	0.8251
	313	37.735	0.0393	0.9907	1.444	1.099	0.9871	−0.1060	8.414	2.171	0.9155
Modified diatomite	298	16.339	0.1348	0.9641	2.030	1.300	0.9949	−0.0779	8.064	2.533	0.8634
	303	14.598	0.1917	0.9830	2.483	1.514	0.9869	−0.0590	8.255	2.911	0.9052
	313	22.026	0.1379	0.9560	2.666	1.258	0.9330	−0.0511	9.656	3.128	0.8549

Fig. 9. Freundlich plots for the adsorption of Zn(II) ions onto natural and modified diatomite at 298 K.

Also the lines supplied from the graphics of ε^2 versus $\ln q_e$ have been given in Fig. 10.

The parameters belonging to the all adsorption isotherm models of Zn(II) for original and modified diatomite were given in Table 1 for three temperatures.

From Table 1, the Langmuir monolayer adsorption capacity, V_m, was large with values between 14.59 and 37.73 mg g^{-1} for natural and modified diatomite. The Langmuir adsorption intensity, K_L, had values of 0.0393–0.1917 L mg^{-1}. The dimensionless separation factor, R_L, had an average value of 0.71 and 0.45 for natural and modified diatomite at 298 K successively, which thus suggests that the favourable adsorption. The n adsorption level was determined from Freundlich adsorption isotherm and while it was 1.124 on original diatomite at 298 K temperature, it was calculated 1.300 on Mn-diatomite. In case of $n = 1$ indicates linear adsorption and equal adsorption energies for all sites. Values of n between 2 and 10 indicate good adsorption. However $n < 1$ shows that the marginal adsorption energy decreases with increasing surface concentration [42,43].

The adsorption energy for natural and modified diatomite at 298 K temperature was found as 1.877 and 2.533 kJ mol^{-1} successively from D–R adsorption isotherm model. The values of adsorption energy increase as the temperature becomes higher.
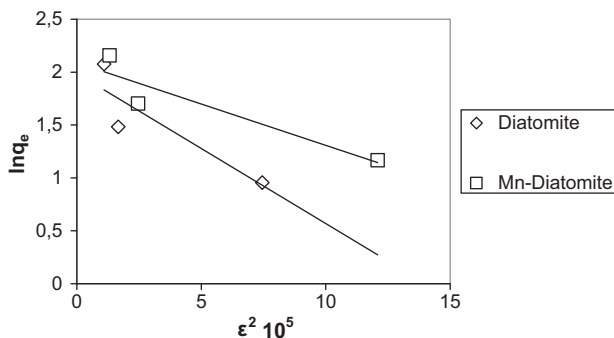
Fig. 10. D–R plots for the adsorption of Zn(II) ions onto natural and modified diatomite at 298 K.
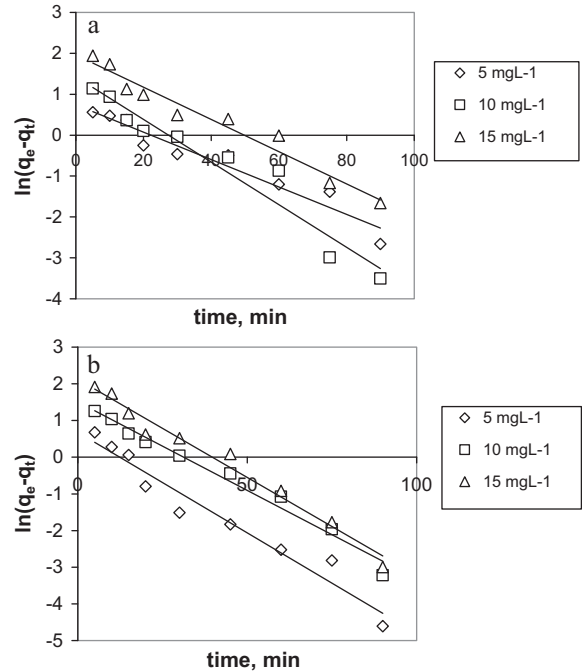

Fig. 11. (a) Pseudo-first order adsorption kinetics of Zn^{2+} onto diatomite at 298 K and (b) pseudo-first order adsorption kinetics of Zn^{2+} onto Mn-diatomite at 298 K.

From the findings of adsorption energy which gives information about the adsorption mechanism like chemical ion exchange or physical adsorption. If the value of E is between 8 and 16 kJ mol^{-1} then the adsorption process follows by chemical ion-exchange and if $E < 8$ kJ mol^{-1} the adsorption process is of a physical nature. Adsorption energy values obtained are below values of a typical ion-exchange process, which thus suggests that the adsorption mechanism is a combination of electrostatic interaction and physical sorption. At the beginning of the binding process (formation of a monolayer), ion-exchange and van der Waals interactions are predominantly responsible for the process [44].

3.4. Adsorption kinetics

The fit of the results of the experimental data to the pseudo-first order, pseudo-second order and intraparticle diffusion models for natural and modified diatomite was carried out, according to Eqs. (10), (12) and (13), respectively. The calculations have been done for 5.10 and 15 mg L^{-1} Zn(II) solution initial concentration at 298 K. The graphic of $\ln(q_e - q_t)$ against t according to pseudo-first-order model has been given in Fig. 11a and b and it is linear. k_1 and q_e can be calculated from the slope and intercept of the plot.

Linear lines obtained from the variation of t/q_t against t according to pseudo-second-order model (Fig. 12a and b). q_e and k_2 rate constants from the slope and intercept have been calculated.
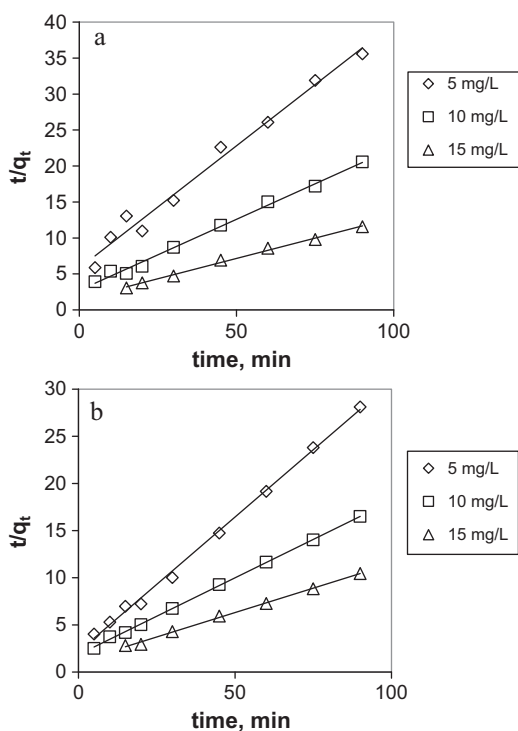
Fig. 12. (a) Pseudo-second-order kinetic plots for the adsorption of Zn(II) ions onto natural diatomite in various initial concentration of zinc solution at 298 K temperature and (b) pseudo-second-order kinetic plots for the adsorption of Zn(II) ions onto Mn-diatomite in various initial concentration of zinc solution at 298 K temperature.
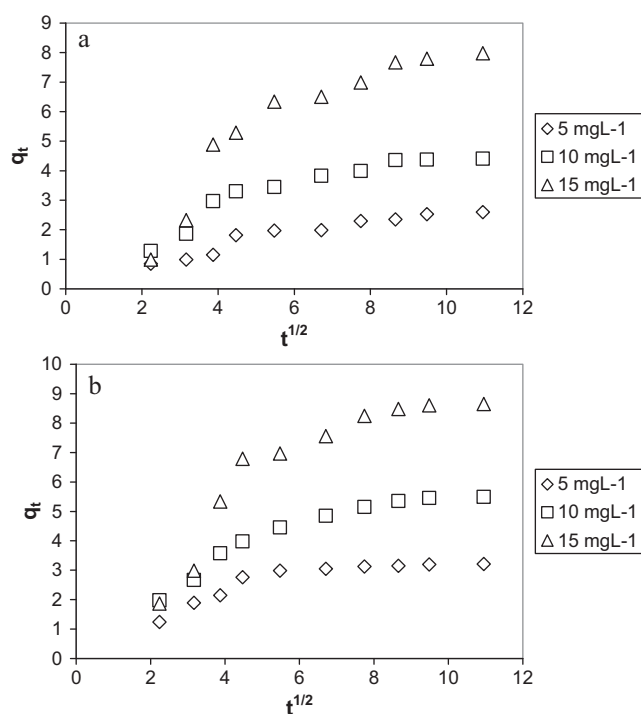

Fig. 13. (a) Two stages of Zn^{2+} adsorption onto diatomite and intraparticle diffusion plot of adsorption of Zn^{2+} onto diatomite at various initial Zn^{2+} concentrations (T = 298 K) and (b) two stages of Zn^{2+} adsorption onto Mn-diatomite and intraparticle diffusion plot of adsorption of Zn^{2+} onto Mn-diatomite at various initial Zn^{2+} concentrations (T = 298 K).

The intraparticle diffusion plot is the plot of amount sorbed per unit weight of sorbent, q_t (mg g^{-1}) versus square root of time, $t^{1/2}$ is shown in Fig. 13a and b for initial Zn^{2+} metal ion concentration of 5, 10 and 15 mg L^{-1} at 298 K.

Fig. 13a and b shows that the adsorption plots are not linear over the whole time range and can be separated into two linear regions which confirm the multi stages of adsorption. The removal of Zn(II) metal ion by adsorption on diatomite was found to be rapid at the initial period of contact time and then become slow and stagnate with increase in contact time. The first stage is characterized by physical adsorption (i.e. ion exchange) at the surface of the diatomite functional group and the second stage is due to the intra-particle diffusion effects [1,18].

Metal ions were transported to the external surface of the diatomite particles through film diffusion and its rate was very fast. After that, metal ions were entered into diatomite particles by intraparticle diffusion through pores. If the intra-particle diffusion is the sole rate-limiting step, it is essential for the q_t versus $t^{1/2}$ plots to go through the origin. However, these plots (Fig. 13a and b) does not fitted with a straight line passing through the origin but also with very poor linear regression coefficients (R^2) indicating the inapplicability of this model and the intra-particle diffusion was not only the rate-controlling step [1]. In the present work (the q_t versus $t^{1/2}$ plots have intercepts in the range 0.53–1.91 mg g^{-1}), it may be concluded that surface adsorption and intra-particle diffusion were concurrently operating during the Zn(II) ions–diatomite interactions [18]. The values of intercept give an idea about the boundary layer thickness such as the larger the intercept, the greater is the boundary layer effect [45].

The kinetic parameters for all experimental data determined by using pseudo-first-order, pseudo-second-order and intraparticle diffusion model have been given in Table 2.

As Table 2, the q_e values calculated from the pseudo-first-order model are match q_e experimental results. However, R^2 values have determined between 0.9383 and 0.9803. When studied on q_e and R^2 values modified from pseudo-second-order model, it has been found that there are similarities between q_e values obtained by experiments and calculations. The R^2 values had been determined between 0.9832 and 0.9994 intervals. It has been shown that, the mechanism concerning adsorption of Zn(II) on natural and modified diatomite can be explained by pseudo-second-order reaction kinetics.

3.5. Thermodynamic parameters of adsorption

The constants of thermodynamics as shown in Table 3 (i.e. Gibbs free energy (ΔG), the change of enthalpy (ΔH) and entropy change (ΔS)). ΔG values are calculated for adsorption of Zn(II) on natural and modified diatomite using Eq. (16). ΔH and ΔS can be determined from the slope and intercept from the plot of $1/T$ versus $\ln K_d$ given in Eq. (15), respectively.

ΔH values for original and Mn-diatomite were determined as 12.28 and 18.30 kJ mol^{-1} successively. ΔH value has positive sign, it was realized that, the adsorption of Zn(II) on original and Mn-diatomite was endothermic. Also the ΔS values calculated from intercept were found by order, 80.12 and 104.65 J K^{-1} mol^{-1} for original and Mn-diatomite. The positive values of entropy may be due to some structural changes in the adsorbate and adsorbents during the adsorption process from aqueous solution onto the adsorbents. In addition, positive value of ΔS indicates the increasing randomness at the solid–liquid interface during the adsorption of Zn^{2+} on the adsorbents [46].

ΔG values are negative for Zinc(II) adsorption on original and Mn-diatomite and these values indicate that adsorption is spontaneous. These values decrease with an increase of temperature. Furthermore, better adsorption is obtained at higher temperature.

Table 2
Intraparticle diffusion, pseudo-first and -second order kinetic parameters of Zn(II) adsorption onto diatomite and Mn-diatomite at various initial Zn(II) concentrations ($T = 298$ K).

Adsorbent	Initial metal concentration (mg L^{-1})	q_e, experimental (mg g^{-1})	Pseudo-first order			Pseudo-second order			Intraparticle diffussion model	
			k_1 (min^{-1})	q_e, calculated (mg g^{-1})	R^2	k_2 (g mg^{-1} min^{-1})	q_e, calculated (mg g^{-1})	R^2	k_i	R^2
Natural diatomite	5	2.60	3.35×10^{-2}	2.09	0.9383	2.00×10^{-2}	2.93	0.9832	0.2103	0.8973
	10	4.41	5.21×10^{-2}	4.16	0.9388	1.43×10^{-2}	5.06	0.9944	0.3392	0.8320
	15	7.98	3.94×10^{-2}	7.08	0.9609	3.06×10^{-3}	8.86	0.9952	0.7379	0.8181
Modified diatomite	5	3.21	5.49×10^{-2}	1.98	0.9529	3.80×10^{-2}	3.50	0.9973	0.2009	0.7307
	10	5.49	4.83×10^{-2}	4.53	0.9803	1.43×10^{-2}	6.14	0.9994	0.3937	0.8684
	15	8.65	5.36×10^{-2}	8.37	0.9770	5.12×10^{-3}	9.66	0.9976	0.7387	0.7886

Table 3
Values of thermodynamic parameters for the adsorption of Zn(II) ions onto natural and Mn-diatomite.

	C_i (mg L^{-1})	ΔH (kJ mol^{-1})	ΔS (J mol^{-1} K^{-1})	ΔG (kJ mol^{-1})		
				298.15 K	303.15 K	313.15 K
Natural diatomite	5	12.28	80.12	−11.59	−11.99	−12.79
	10	20.85	106.07	−10.76	−11.29	−12.35
	15	5.65	58.26	−11.71	−12.00	−12.59
Modified diatomite	5	18.30	104.65	−12.88	−13.41	−14.45
	10	18.55	102.25	−11.92	−12.43	−13.45
	15	25.99	127.44	−11.98	−12.62	−13.89

4. Conclusions

In the sorption studies conducted on natural and modified diatomite resulted in the following salient points.

(1) The sorption of Zn(II) on the natural and modified diatomite was an endothermic processes, controlled by physical mechanisms and spontaneously. The adsorption characteristics of zinc metal ion are strongly affected by initial metal ion concentration and temperature, respectively. The adsorption efficiency with modified diatomite was greater than natural diatomite.

(2) Kinetic experiments clearly indicate that adsorption of zinc metal ion on diatomite samples is more or less a two step process: a rapid adsorption of zinc metal ion to the external surface followed by intraparticle diffusion into the interior of adsorbent which has also been confirmed by intraparticle diffusion model.

As the experimental data has been applied on the kinetic models, it was found that, the adsorption of Zn(II) on natural and modified diatomite could be explained by the mechanism of pseudo-second-order.

(3) The experimental data were applied on Langmuir, Freundlich and D–R isotherm models. For natural and modified diatomite, these models were fitted well. The values of adsorption energy calculated from D–R adsorption isotherm. E (kJ mol^{-1}) show that the adsorption mechanism of Zn(II) on natural and modified diatomite is a combination of electrostatic interaction and physical sorption. Besides the enthalpy of sorption for each diatomite samples are lower than 40 kJ mol^{-1} indicating that the sorption processes were controlled by physical mechanism rather than chemical mechanism. The heat of physical adsorption involves relatively weak intermolecular forces such as van der Waals and mainly electrostatic interaction. The constant value, R_L (low separation factor) in Langmuir isotherm gives an indication of favourable adsorption.

References

[1] F. Arias, T.K. Sen, Removal of zinc metal ion (Zn^{2+}) from its aqueous solution by kaolin clay mineral: a kinetic and equilibrium study, Colloid Surface A 348 (2009) 100–108.
[2] T. Fan, Y. Liu, B. Feng, G. Zeng, C. Yang, M. Zhou, H. Zhou, Z. Tan, X. Wang, Biosorption of cadmium(II), zinc(II) and lead(II) by penicillium simplicissimum: isotherms, kinetics and thermodynamics, J. Hazard. Mater. 160 (2008) 655–661.
[3] H. Ucun, O. Aksakal, E. Yildiz, Copper (II) and zinc(II) biosorption on *Pinus sylvestris* L., J. Hazard. Mater. 161 (2009) 1040–1045.
[4] X. Tang, Z. Li, Y. Chen, Adsorption behavior of Zn(II) on calcinated Chinese loess, J. Hazard. Mater. 161 (2009) 824–834.
[5] S. Veli, B. Alyuz, Adsorption of copper and zinc from aqueous solutions by using natural clay, J. Hazard. Mater. 149 (2007) 226–233.
[6] S.H. Lin, R.S. Juang, Heavy metal removal from water by sorption using surfactant-modified montmorillonite, J. Hazard. Mater. 92 (2002) 315–326.
[7] K.G. Bhattacharyya, S. Sen Gupta, Kaolinite and montmorillonite as adsorbents for Fe(III), Co(II) and Ni(II) in aqueous medium, Appl. Clay Sci. 41 (2008) 1–9.
[8] Y. Orhan, H. Buyukgungor, The removal of heavy metals by using agricultural wastes, Water Sci. Technol. 28 (1993) 247–255.
[9] M. Aivalioti, I. Vamvasakis, E. Gidarakos, BTEX and MTBE adsorption onto raw and thermally modified diatomite, J. Hazard. Mater. 178 (2010) 136–143.
[10] J.F. Lemonas, Diatomite, Am. Ceram. Soc. Bull. 76 (1997) 92–95.
[11] M.A. Al-Ghouti, M.A.M. Khraisheh, M. Tutunji, Flow injection potentiometric stripping analysis for study of adsorption of heavy metal ions onto modified diatomite, Chem. Eng. J. 104 (2004) 83–91.
[12] E. Erdem, G. Çölgecen, R. Donat, The removal of textile dyes by diatomite earth, J. Colloid Interface Sci. 282 (2005) 314–319.
[13] L.T. Zhuravlev, The surface chemistry of amorphous silica. Zhuravlev model, Colloid Surface A 173 (2000) 1–38.
[14] M.A. Al-Ghouti, Y.S.M. Al-Degs, A.M. Khraisheh, M.N. Ahmad, S.J. Allen, Mechanisms and chemistry of dye adsorption on manganese oxides-modified diatomite, J. Environ. Manage. 90 (2009) 3520–3527.
[15] Y. Al-Degs, M.A.M. Khraısheh, M.F. Tutunji, Sorption of lead ions on diatomite and manganese oxides modified diatomite, Water Res. 35 (2001) 3724–3728.
[16] G.W. Sears, Determination of specific surface area of colloidal silica by titration with sodium hydroxide, Anal. Chem. 28 (1956) 1981–1983.
[17] N. Fiol, I. Villaescusa, Determination of sorbent point zero charge: usefulness in sorption studies, Environ. Chem. Lett. 7 (2009) 79–84.
[18] K.G. Bhattacharyya, A. Sharma, Kinetics and thermodynamics of methylene blue adsorption on Neem (*Azadirachta indica*) leaf powder, Dyes Pigments 65 (2005) 51–59.
[19] M.M. Dubinin, The potential theory of adsorption of gases and vapors for adsorbents with energetically nonuniform surfaces, Chem. Rev. 60 (1960) 23.
[20] R.A. Shawabkeh, M.F. Tununji, Experimental study and modeling of basic dye sorption by diatomaceous clay, Appl. Clay Sci. 24 (2003) 111–120.
[21] Z. Al-Qodah, W.K. Lafi, Z. Al-Anber, M. Al-Shannag, A. Harahsheh, Adsorption of methylene blue by acid and heat treated diatomaceous silica, Desalination 217 (2007) 212–224.

[22] A.A.M. Daifullah, B.S. Girgis, Impact of surface characteristics of activated carbon on adsorption of BTEX, Colloid Surface A 214 (2003) 181–193.

[23] W.T. Tsai, K.J. Hsien, Y.M. Chang, C.C. Lo, Removal of herbicide paraquat from an aqueous solution by adsorption onto spent and treated diatomaceous earth, Bioresour. Technol. 96 (2005) 657–663.

[24] W.T. Tsai, C.W. Lai, T.Y. Su, Adsorption of bisphenol-A from aqueous solution onto minerals and carbon adsorbents, J. Hazard. Mater. B134 (2006) 169–175.

[25] Y.S. Ho, G. McKay, Pseudo-second order model for sorption processes, Process. Biochem. 34 (1999) 451–465.

[26] A.R. Kul, N. Caliskan, Equilibrium and kinetic studies of the adsorption of Zn(II) ions onto natural and activated kaolinites, Adsorpt. Sci. Technol. 27 (2009) 85–105.

[27] G. Sheng, S. Wang, J. Hu, Y. Lu, J. Li, X. Dong, Y. Wang, Adsorption of Pb(II) on diatomite as affected via aqueous solution chemistry and temperature, Colloid Surface A 339 (2009) 159–166.

[28] M.A. Khraisheh, M.A. Al-Ghouti, S.J. Allen, M.N. Ahmad, Effect of OH and silanol groups in the removal of dyes from aqueous solution using diatomite, Water Res. 39 (2005) 922–932.

[29] B. Bahramian, F.D. Ardejani, V. Mirkhani, K. Badii, Diatomite supported manganese Schiff base: an efficient catalyst for oxidation of hydrocarbons, Appl. Catal. A: Gen. 345 (2008) 97–103.

[30] N. Çalışkan, E. Söğüt, C. Saka, Y. Yardım, Z. Şentürk, The natural diatomite from Çaldıran-Van (Turkey): electroanalytical application to antimigraine compound naratriptan at modified carbon paste electrode, Comb. Chem. High Throughput Screen. 13 (2010) 703–711.

[31] J. Luo, Q. Zhang, S.L. Suib, Mechanistic and kinetic studies of crystallisation of birnessite, Inorg. Chem. 39 (2000) 741–747.

[32] B. Yılmaz, N. Ediz, The use of raw and calcined diatomite in cement production, Cement Concrete Comp. 30 (2008) 202–211.

[33] W. Zhi-Ying, Z. Li-Ping, Y. Yu-Xiang, Structural investigation of some important Chinese diatomites, Glass Phys. Chem. 35 (2009) 673–679.

[34] R. Köseoglu, F. Köksal, E. Çiftci, M. Akkurt, Identification of paramagnetic radicals in γ-irradiated natural diatomite minerals by electron paramagnetic resonance, J. Mol. Struct. 733 (2005) 151–154.

[35] G. Zhang, Y. Liu, Y. Xie, X. Yang, B. Hu, S. Ouyang, H. Liu, H. Wang, Zinc adsorption on Na-rectorite and effect of static magnetic field on the adsorption, Appl. Clay Sci. 29 (2005) 15–21.

[36] P. Srivastava, B. Singh, M. Angove, Competitive adsorption behavior of heavy metals on kaolinite, J. Colloid Interface Sci. 290 (2005) 28–38.

[37] M.A. Al-Ghouti, M.A.M. Khraisheh, S.J. Allen, M.N. Ahmad, The removal of dyes from textile wastewater: a study of the physical characteristics and adsorption mechanisms of diatomaceous earth, J. Environ. Manage. 69 (2003) 229–238.

[38] M.A. Al-Ghouti, M.A.M. Khraisheh, M.N.M. Ahmad, S. Allen, Adsorption behaviour of methylene blue onto Jordanian diatomite: a kinetic study, J. Hazard. Mater. 165 (2009) 589–598.

[39] P. Miretzky, C. Muñoz, E. Cantoral-Uriza, Cd^{2+} adsorption on alkaline-pretreated diatomaceous earth: equilibrium and thermodynamic studies, Environ. Chem. Lett. 9 (2011) 55–63.

[40] J.W. Murray, The surface chemistry of hydrous manganese dioxide, J. Colloid Interface Sci. 46 (1974) 357–371.

[41] M. Jiang, Q. Wang, X. Jin, Z. Chen, Removal of Pb(II) from aqueous solution using modified and unmodified kaolinite clay, J. Hazard. Mater. 170 (2009) 332–339.

[42] H. Koyuncu, A.R. Kul, N. Yıldız, A. Çalımlı, H. Ceylan, Equilibrium and kinetic studies for the sorption of 3-methoxybenzaldehyde on activated kaolinites, J. Hazard. Mater. 141 (2007) 128–139.

[43] Ş. Kubilay, R. Gürkan, A. Savran, T. Şahan, Removal of Cu(II), Zn(II) and Co(II) ions from aqueous solutions by adsorption onto natural bentonite, Adsorption 13 (2007) 41–51.

[44] W. Mrozik, C. Jungnickel, M. Skup, P. Urbaszek, P. Stepnowski, Determination of the adsorption mechanism of imidazolium-type ionic liquids onto kaolinite: implications for their fate and transport in the soil environment, Environ. Chem. 5 (2008) 299–306.

[45] A.S. Ozcan, B. Erdem, A. Ozcan, Adsorption of acid blue 193 from aqueous solutions onto BTMA-bentonite, Colloid Surface A 266 (2005) 73–81.

[46] E.I. Unuabonah, K.O. Adebowale, B.I. Olu-Owolabi, Kinetic and thermodynamic studies of the adsorption of lead (II) ions onto phosphate-modified kaolinite clay, J. Hazard. Mater. 144 (2007) 386–395.